1   Multiple mechanisms impact fluconazole resistance of mutant Erg11 proteins in

2   *Candida glabrata*

3

4

5   Bao Gia Vu and W. Scott Moye-Rowley[*]

6

7   Running title: Cellular effects of Erg11 mutants

8

9

10

11

12   From: Department of Molecular Physiology and Biophysics, Carver College of Medicine,

13   University of Iowa, Iowa City, IA 52242 USA.

14

15

16   [*]Corresponding author. E-mail: scott-moye-rowley@uiowa.edu

17

18   Revised draft: September 2, 2021

19

20   Abstract (247 words)

21   Azoles, the most commonly used antifungal drugs, specifically inhibit the fungal lanosterol α-14

22   demethylase enzyme, which is referred to as Erg11. Inhibition of Erg11 ultimately leads to a

23   reduction in ergosterol production, an essential fungal membrane sterol. Many *Candida*

24   species, such as *Candida albicans*, develop mutations in this enzyme which reduces the azole

25   binding affinity and results in increased resistance. *Candida glabrata* is also a pathogenic yeast

26   that has low intrinsic susceptibility to azole drugs and easily develops elevated resistance.

27   These azole resistant mutations typically cause hyperactivity of the Pdr1 transcription factor and

28   rarely lie within the *ERG11* gene. Here, we generated *C. glabrata ERG11* mutations that were

29   analogous to azole resistance alleles from *C. albicans ERG11*. Three different Erg11 forms

30   (Y141H, S410F, and the corresponding double mutant (DM)) conferred azole resistance in *C.*

31   *glabrata* with the DM Erg11 form causing the strongest phenotype. The DM Erg11 also induced

32   cross-resistance to amphotericin B and caspofungin. Resistance caused by the DM allele of

33   *ERG11* imposed a fitness cost that was not observed with hyperactive *PDR1* alleles. Crucially,

34   the presence of the DM *ERG11* allele was sufficient to activate the Pdr1 transcription factor in

35   the absence of azole drugs. Our data indicate that azole resistance linked to changes in

36   *ERG11* activity can involve cellular effects beyond an alteration in this key azole target enzyme.

37   Understanding the physiology linking ergosterol biosynthesis with Pdr1-mediated regulation of

38   azole resistance is crucial for ensuring the continued efficacy of azole drugs against *C. glabrata*.

39

40   Importance (136 words)

41   Azole drugs target the Erg11 enzyme and lead to a reduction in fungal ergosterol, a vital sterol

42   in yeast. Mutations in Erg11 are common among azole resistant *Candida albicans* clinical

43   isolates, but not in *C. glabrata*, a major human pathogen. In this study, we showed that *ERG11*

44   mutations were tolerated in *C. glabrata*, and these mutations could confer azole resistance. We

45   found that the strongest azole-resistant allele of *ERG11* led to induction of the Pdr1 transcription

46 factor and Cdr1 ATP-binding cassette transporter protein in the absence of drug. *ERG11*

47 mutations can cause azole resistance via altered enzymatic properties but also by triggering

48 induction of other resistance systems owing to impacts on ergosterol biosynthesis. These data

49 illustrate the deep connections between ergosterol biosynthesis and regulation of membrane

50 transporter proteins via Pdr1 and the ergosterol-responsive transcription factor Upc2A.

51

52 Introduction

53   Ergosterol is essential for fungal plasma membrane homeostasis (1, 2). It maintains

54 membrane integrity and fluidity, as well as facilitates membrane-bound enzymatic reactions (1).

55 The azole class of antifungal therapy targets the fungal ability to synthesize ergosterol through

56 inhibition of the function of lanosterol 14-alpha-demethylase, which is encoded by the *ERG11*

57 gene (3) (4). The Erg11 enzyme catalyzes a three-step reaction that results in the

58 demethylation of lanosterol. In each step, one oxygen molecule is oxidized, leading to the

59 production of one NADPH molecule (4, 5). The nucleophilic N-4 atom of the azole ring binds to

60 heme, while the N-1 group interacts with the enzyme active site, directly competing with the

61 normal substrate (lanosterol) binding (6, 7). While azoles bind selectively to the Erg11 enzyme

62 (8) the affinity of this enzyme for different azoles varies; with fluconazole binding with lower

63 affinity than either itraconazole or voriconazole (4).

64   In *Candida albicans* (Ca), mutations in the Erg11 enzyme have been shown to alter

65 azole binding capacity and significantly reduce the drug inhibitory effect resulting in an

66 enhanced azole resistant phenotype (9-14)}. The majority of these mutations cluster into three

67 hot spots, located within residues 105 to 165, 266 to 287, and 405 to 488 (15). The ability to

68 confer azole resistance by some of these mutations has also been confirmed by introducing

69 these mutations on plasmids into a heterologous *Saccharomyces cerevisiae* system and then

70 assessing azole susceptibility. With this approach, single amino acid mutations, such as:

71 Y132H, S405F, G464S, R467K, and double mutations, such as: Y132H with S405F, Y132H with

3

72   G464S, R467K with G464S have been shown to confer azole resistance in *S. cerevisiae* (9). In

73   addition, several *CaERG11* constructs of the enzyme catalytic domain containing amino acid

74   substitutions, including Y132H, F145L, I471T, S279F, and G464S have been expressed in

75   *Escherichia coli*, purified, and showed to exhibit a lower binding capacity to azoles (15). Finally,

76   many of these mutant alleles have also been introduced back into an azole-susceptible *C.*

77   *albicans* strain, at the *ERG11* gene native locus, to confirm the relative contributions of

78   individual and combined mutation to azole resistance (10).

79   Unlike in *C. albicans*, mutations in the *ERG11* gene have been rarely reported among

80   *Candida glabrata* azole resistant clinical isolates. The most common amino acid substitution

81   mutations in *C. glabrata* are in the gene encoding a Zn_2Cys_6 zinc cluster-containing transcription

82   factor called Pdr1 (16). These mutations yield a gain-of-function (GOF) phenotype and lead to

83   the elevated transcription of downstream target genes, such as the ATP-binding cassette (ABC)

84   transporter-encoding *CDR1* gene. The Cdr1 transporter is required for the azole resistant

85   mechanism in both wild-type and GOF *PDR1 C. glabrata* isolates (17).

86   We recently reported that there is biological crosstalk between the ergosterol

87   biosynthesis pathway and the drug efflux pump system in *C. glabrata* (18). Alteration in

88   ergosterol synthesis directly induced expression of both Pdr1 and Cdr1. The Zn_2Cys_6 zinc

89   cluster-containing factor Upc2A is essential for such cross-interaction, through its functions as a

90   master transcription factor regulating the expression levels of both ergosterol synthesis genes

91   (*ERG*) and *PDR1-CDR1* genes (19) (20) . Since our earlier experiments indicated that activity of

92   the Pdr1/*CDR1* system was responsive to ergosterol biosynthesis, we further wanted to

93   determine if mutations in *ERG11* that reduced azole susceptibility might act via induction of this

94   separate azole resistance pathway. Considering the conserved inhibitory effects of azoles on

95   the Erg11 protein in both *C. albicans* and *C. glabrata*, we first generated isogenic *C. glabrata*

96   isolates carrying mutant *ERG11* alleles, analogs of the *CaERG11* Y132H, S405F or Y132H-

97   S405F mutations. Then we examined the effects of these mutant alleles on ergosterol

4

98   synthesis, antifungal drug resistance, and abilities to cross-regulate the drug efflux pump Pdr1-

99   Cdr1 system. Our data indicate that azole-resistant *ERG11* mutations can activate function of

100   Pdr1 with attendant induction of genes (like *CDR1*) downstream of this factor, even in the

101   absence of drug. These findings illustrate the importance of considering secondary effects of

102   *ERG11* mutations on activation of other resistance pathways when evaluating the azole

103   resistance caused by these lesions. Our data provide further evidence directly tying expression

104   of the Pdr1-dependent resistance pathway to ergosterol biosynthesis.

105

106   Results

107

108   **Generation of azole-resistant forms of *C. glabrata* Erg11.** Detailed structural information is

109   available for the Erg11 enzymes from these two pathogenic *Candida* species as their three

110   dimensional structures have recently been solved by X-ray crystallography, along with the

111   previously determined structure of *S. cerevisiae* Erg11 (6, 21). Figure 1A shows an alignment of

112   the amino acid sequences of these three closely related proteins.

113   Previous analyses of azole resistant clinical isolates of *C. albicans* identified changes in

114   residue tyrosine 132 to histidine (Y132H), serine 405 to phenylalanine (S405F) and a double

115   mutant containing both of these lesions (Y132H S405F, referred to as double mutant or DM

116   here) to trigger a decrease in fluconazole susceptibility when present in the *C. albicans* Erg11

117   enzyme (9). Inspection of the aligned sequences shown in Figure 1A indicated that both Y141

118   and S410 (in *C. glabrata*) were conserved residues across the enzymes from *S. cerevisiae* and

119   the two *Candida* species. To determine if these same substitution mutations would cause

120   similar fluconazole resistance phenotypes when introduced into the *C. glabrata* Erg11, we used

121   site-directed mutagenesis to generate the appropriate mutant enzymes. These were returned to

122   *C. glabrata* as the sole source of Erg11 using a plasmid shuffling approach (see Materials and

123   Methods). Appropriate transformants were tested for their resistance to fluconazole,

124   caspofungin and amphotericin B (Figure 1B).

125   The presence of either single mutant form of Erg11 (Y141H or S410F) led to a slight

126   increase in fluconazole resistance compared to the wild-type enzyme while the double mutant

127   (Y141H and S410F: DM) caused the strongest elevation in fluconazole resistance. The

128   enhanced effect on azole resistance caused by combining these two mutations into a single

129   enzyme has been seen before (9). Only the DM Erg11 was able to enhance resistance to

130   caspofungin or amphotericin B. These data indicated that these mutant forms of *C. glabrata*

131   Erg11 were able to increase fluconazole resistance like their *C. albicans* counterparts and,

132   when combined in the DM Erg11, increased resistance to two other antifungal drugs. We also

133   tested these strains for their susceptibility to voriconazole and itraconazole (Supplemental

134   Figure 1) and found that the mutants caused voriconazole phenotypes similar to those seen for

135   fluconazole but had no significant effect on itraconazole susceptibility. This differential response

136   of a given *ERG11* mutant to different azole drugs has been observed previously (9, 22), with

137   relatively large effects on FLC resistance not correlating with a similar effect to itraconazole

138   susceptibility.

139   The multidrug resistant nature of the DM *ERG11* mutant strain was not expected. This

140   finding prompted us to evaluate the levels of ergosterol supported by each of these mutant

141   strains as well as expression of genes that could explain the increased resistance to

142   caspofungin. The three mutant strains along with their wild-type *ERG11* counterpart were grown

143   to mid-log phase and allowed to grow for 3 or 24 hours with or without fluconazole challenge.

144   Total sterols were extracted from these cultures and assayed for the level of ergosterol

145   produced in each strain. Total RNA was also prepared from isogenic wild-type and DM *ERG11*

146   strains without fluconazole challenge and assayed by RT-qPCR for the mRNA levels of the

147   genes indicated.

148   Ergosterol levels were the lowest in the DM Erg11-expressing strains in the absence of

149   fluconazole stress (Figure 2A). The two single mutants produced ergosterol levels that were

150   very similar to those seen in the wild-type strain. A 3 hour treatment with fluconazole caused a

151   dramatic change in relative ergosterol levels as at this point, the DM Erg11 strain had the

152   highest level of ergosterol while the other 3 strains dropped below this level (Figure 2B). No

153   differences were observed between the two mutant forms of Erg11 compared to the wild-type

154   protein until the fluconazole treatment was extended to 24 hours (Figure 2C). At this time, the

155   DM Erg11 still produced the highest level of ergosterol but now both the Y141H and S410F

156   single mutant strains had levels of ergosterol that were higher than the wild-type but still lower

157   than the DM Erg11.

158   Analysis of mRNA levels from genes directly involved in production of β-glucan synthase

159   (*FKS1*, *FKS2*, *FKS3*, *KNH1*) as well as regulators of these genes (*CRZ1*, *CNA1*) indicated that

160   only the mRNA for the *FKS2* gene was elevated in the DM *ERG11* mutant compared to its

161   cognate wild-type strain (Figure 2D). This transcriptional induction of *FKS2* could serve to

162   explain the increase in caspofungin resistance seen in the DM Erg11-expressing strain.

163   We analyzed the contribution of the Crz1 transcription factor to the DM Erg11-triggered

164   increase in caspofungin resistance by disrupting this gene in both wild-type and the isogenic DM

165   *ERG11* strains (Figure 2E). At low concentrations of caspofungin, DM Erg11 was still able to

166   increase drug resistance in a *crz1Δ* strain compared to the wild-type *ERG11* (see 50 ng/ml

167   plate). However, loss of Crz1 eliminated high level (100 ng/ml) caspofungin resistance. We

168   interpret these data to suggest there are at least two effects of the DM *ERG11* allele on

169   caspofungin resistance: a minor one that is Crz1 independent and a major one that requires the

170   presence of Crz1.

171

172 **Communication between *ERG11* and Pdr1/*CDR1* pathway.** Our previous work

173 demonstrated that reduction in Erg11 expression led to an induction of the Pdr1 transcription

174 factor and its target genes such as *CDR1* (19) . To determine if these mutant forms of Erg11

175 triggered a similar response, we measured expression of Pdr1 and Cdr1 at both the protein and

176 mRNA levels. Transformants containing the various *ERG11* alleles were grown to mid-log

177 phase and either treated with fluconazole for 3 hours or left untreated. Total RNA was prepared

178 from these cultures and mRNA for *CDR1*, *PDR1* and *ERG11* measured by RT-qPCR (Figure

179 3A).

180 In the absence of fluconazole stress, only the DM *ERG11* allele led to induction of all

181 three of these mRNAs. Upon challenge with fluconazole, all of these genes were induced to

182 similar relative levels. The enhanced fluconazole resistance seen in the DM *ERG11* strain may

183 be explained by elevated *PDR1* and *CDR1* transcription, at least in part.

184 The levels of these proteins were also evaluated by western blots using appropriate

185 rabbit polyclonal antibodies for each *C. glabrata* protein (Figure 3B) and quantitated (Figure 3C).

186 Both Pdr1 and Cdr1 were elevated in untreated cells along with Erg11 in the DM *ERG11* strain.

187 Treatment with fluconazole led to similar levels of induction of all these proteins. Upc2A protein

188 levels were not changed under any of these conditions or genetic backgrounds. This is

189 consistent with Upc2A regulation occurring at the post-translational step as has been suggested

190 (23-25) .

191 The levels of mRNA of a range of genes in the ergosterol biosynthetic pathway were

192 also determined in both the DM and wild-type Erg11 strains (Figure 3D). These data are

193 presented as a ratio of mRNA level in the DM Erg11 strain over the wild-type level for each

194 transcript. Most of these *ERG* genes were induced at least 2-fold in the DM Erg11-expressing

195 cells, consistent with the ergosterol limitation in this strain although several *ERG* genes

196 including *ERG9*, *ERG7*, *ERG10* and *HMG1* showed little to no increase. Clearly, the presence

197 of the DM Erg11 enzyme induced a wide range of transcriptional activation across the

8

198   ergosterol pathway in addition to its effects on *PDR1* and *CDR1* expression. We also suggest

199   that the DM *ERG11* strain may activate Crz1 leading to the previously observed increase in

200   *FKS2* expression and caspofungin resistance. These effects on Pdr1 and Crz1 would explain

201   the multidrug resistance seen in DM *ERG11* mutant strains.

202

203   **Upc2A function is increased in the *ERG11* mutants**. Our previous data showed that genetic

204   inhibition of *ERG11* gene expression could induce the expression of the drug efflux pump

205   system Pdr1-Cdr1 (19). Upc2A was essential for this interaction in which it directly induced the

206   expression levels of genes in both the *ERG* and Pdr1/*CDR1* pathways (19, 20). Since these two

207   pathways were also induced in the DM *ERG11* mutant, we wanted to determine if Upc2A

208   function was activated in response to these changes in the *ERG11* gene. To test this, we

209   generated an Upc2A reporter construct that contains five copies of the Upc2A binding site

210   (Sterol Response Element: SRE) from the *ERG1* promoter. These concatemerized SREs were

211   placed upstream from the *S. cerevisiae CYC1* promoter that was fused to *E. coli lacZ.* To

212   confirm that this reporter system was sensitive to the *UPC2A* allele, we introduced this plasmid

213   into isogenic *C. glabrata* strains containing the 3X HA-*UPC2A*, 3X HA-G898D *UPC2A* gain-of-

214   function mutation (20) or a null allele of *UPC2A*. A plasmid containing only the *CYC1-lacZ*

215   fusion gene with no upstream activation sequence was also used as negative control (Figure

216   4A).

217   The introduction of the gain-of-function form of Upc2A (G898D *UPC2A*) led to production

218   of the highest level of β-galactosidase seen from the 5X SRE-*CYC1-lacZ* plasmid with nearly

219   1200 Miller units of activity compared to approximately 800 Miller units when the wild-type

220   *UPC2A* gene was present. Loss of *UPC2A* lowered expression to approximately 80 Miller units.

221   All *C. glabrata* isolates carrying the *CYC1-lacZ* control plasmid lacking an upstream activation

222   sequence showed minimal levels of β-galactosidase activity. These data are consistent with

223   this reporter system faithfully detecting the status of the *UPC2A* gene.

224   Next, we transformed these two plasmids into strains containing the various *ERG11*

225   alleles. Appropriate transformants were grown to mid-log phase and enzyme levels determined

226   (Figure 4B). The highest level of β-galactosidase activity was produced in the presence of the

227   DM *ERG11* allele, consistent with this strain triggering the highest level of Upc2A activity. Both

228   single mutant *ERG11* alleles induced smaller but significant increases in expression of the 5X

229   SRE-*CYC1-lacZ* plasmid compared to the wild-type *ERG11*-containing strain. Only minimal

230   levels of β-galactosidase activity were produced in strains containing the *CYC1-lacZ* reporter

231   plasmid lacking any SREs as upstream control elements. These data support the view that the

232   DM *ERG11* allele caused the largest increase in Upc2A function, likely through production of the

233   most compromised form of the Erg11 enzyme, but each single mutant had a less dramatic but

234   still detectable impact on Upc2A. To directly assess Upc2A function, we carried out single gene

235   chromatin immunoprecipitation analysis of Upc2A binding to target promoters

236   Previous work from several labs including ours (20, 25) has provided evidence that

237   ergosterol limitation increased Upc2A DNA-binding to nuclear target genes. We also found that

238   these Upc2A target genes included the *PDR1* and *CDR1* genes (19), linking control of

239   ergosterol biosynthesis with expression of genes involved in drug resistance. To determine if

240   the presence of the fluconazole-resistant, DM allele of *ERG11* caused increased levels of

241   Upc2A DNA binding, chromatin immunoprecipitation was used to detect binding of this factor to

242   SREs present in the *ERG11*, *CDR1* and *PDR1* promoters. Non-specific binding was also

243   evaluated by examining Upc2A enrichment on the HO promoter and *ERG11* coding sequence.

244   Isogenic wild-type and DM *ERG11* strains were grown to mid-log phase and Upc2A DNA-

245   binding analyzed by ChIP using anti-Upc2A or a non-specific control polyclonal antiserum

246   (Figure 4C).

247   Upc2A binding to the *ERG11* SRE was strongly induced when cells contained the DM

248 *ERG11* allele compared to the wild-type gene. Upc2A association with the *PDR1* SRE was also

249 induced under these conditions although binding to *CDR1* did not change. Control ChIP

250 reactions confirmed that the Upc2A binding was antibody-specific and showed no enrichment

251 with either the *HO* gene or the *ERG11* coding sequence. The increased Upc2A-dependent

252 transcriptional activation and DNA-binding indicate that Upc2A function was increased in strains

253 containing the DM *ERG11* allele compared to the wild-type gene.

254

255 **Phenotypic comparison of *PDR1* GOF and DM *ERG11* mutations indicate mutant Pdr1**

256 **factors drive higher level azole resistance.** Since the DM *ERG11* mutant was capable of

257 inducing strong fluconazole resistance, we wanted to compare its behavior to that seen in the

258 presence of *PDR1* GOF alleles. These GOF mutants of *PDR1* represent the vast majority of

259 azole resistant mutants found in *C. glabrata* isolates (26-28). An isogenic series of strains was

260 produced that produced wild-type or DM mutant forms of Erg11 containing the following alleles

261 of *PDR1*: *pdr1Δ,* wild-type, D1082G or R376W. These strains were grown to mid-log phase and

262 tested for their relative susceptibility to 30 μg/ml fluconazole in a serial dilution plate assay

263 (Figure 5A).

264   Both GOF forms of *PDR1* lowered fluconazole susceptibility more than the DM *ERG11*

265 strain. To probe the relative effects of mutations in either *PDR1* or *ERG11*, we carried out a

266 competitive growth assay in which equal numbers of cells containing mutations of interest were

267 mixed together. These mixed cultures were then allowed to grow in the presence or absence of

268 fluconazole challenge and the relative contribution of each mutant strain to the final population

269 determined. This competitive growth assay allows subtle differences to be more readily

270 detected than on a plate-based assay.

11

271   We prepared mixed cultures of isogenic wild-type and DM *ERG11* cells (Figure 5B) and

272   allowed these cultures to grow under untreated conditions (YPD) or in YPD medium containing

273   fluconazole to late log phase. Growth in rich medium led to an increase in the population of the

274   wild-type (60% final) compared to the DM *ERG11* strain (40% final). This analysis indicated that

275   the DM *ERG11* had a growth defect compared to wild-type cells in the absence of fluconazole

276   but this mutant allele conferred a significant growth advantage in the presence of this drug.

277   The relative growth of the DM *ERG11* strain was then compared to each of the *PDR1*

278   GOF mutant strains (Figures 5C and 5D). In both cases, the GOF *PDR1* mutant outcompeted

279   the DM *ERG11* strain in the presence of fluconazole (D1082G-74%: DM-26%; R376W-65%:

280   DM-35%) while the only difference in growth in the absence of drug was seen in comparison of

281   the D1082G *PDR1* strain compared to the DM *ERG11*: 58% to 42%, respectively. Both GOF

282   *PDR1* mutants were more effective in conferring fluconazole resistance while growing at least

283   as well (R376W) if not better (D1082G) than the DM *ERG11* strain. While we are only testing a

284   single mutant form of *ERG11* here, growth differences associated with azole-resistant forms of

285   Erg11 may help explain the predominance of GOF mutants of *PDR1* in clinical azole-resistant

286   isolates of *C. glabrata*.

287

288   **Increased activation of *PDR1* and *CDR1* transcription seen in presence of GOF *PDR1***

289   **mutants compared to DM *ERG11*.** The phenotypic data above indicated that both GOF *PDR1*

290   strains produced a stronger effect on fluconazole resistance than the presence of the DM

291   *ERG11* allele. To probe the basis of this phenotypic difference, we examined transcription of

292   *CDR1*, *PDR1* and *ERG11* by RT-qPCR. Strains containing wild-type, D1082G or R376W forms

293   of *PDR1* or the DM *ERG11* were grown to mid-log phase in the absence or presence of

294   fluconazole. Levels of mRNA from these three genes were assayed as before.

295   *CDR1* mRNA levels were strongly elevated in the presence of both GOF *PDR1*

296   mutations, well above those induced by the presence of the DM *ERG11* mutation (Figure 6A).

12

297   This increase was seen both in the absence as well as the presence of fluconazole. *PDR1*

298   mRNA levels were significantly higher in the presence of the two GOF alleles than in the DM

299   *ERG11* but this difference was restricted to the absence of fluconazole. Drug treatment

300   elevated both wild-type and DM *ERG11* strains to levels similar to those of the GOF mutants.

301   Finally, *ERG11* mRNA levels were higher in the DM *ERG11* strain than in the other three strains

302   in the absence of fluconazole. Strikingly, fluconazole exposure induced *ERG11* mRNA to

303   higher levels in the strains containing wild-type *PDR1* but was less effective in the two GOF

304   *PDR1*-containing strains. These data suggest that the increased *PDR1*/*CDR1* expression seen

305   in the GOF *PDR1* strains may reduce the level of fluconazole stress (and associated *ERG11*

306   induction) seen. The changes seen in mRNA levels were well-correlated with western blot

307   analyses for each protein (Figures 6B and 6C). Upc2A protein levels were constant under all

308   conditions tested, consistent with changes due to this factor being caused by alterations in

309   Upc2A function rather than its expression.

310

311   **Reduced levels of Upc2A exacerbate the growth defect of the DM *ERG11* strain.** Our

312   analysis of the cellular response to the presence of the DM *ERG11* mutation demonstrated the

313   involvement of Upc2A as activity of this factor was induced in this genetic background

314   compared to wild-type cells. We introduced the highly repressible *MET3* promoter (29) in place

315   of the chromosomal *UPC2A* cognate region in order to test the effect of changing Upc2A

316   production via repression in the presence of exogenous methionine. This *MET3-UPC2A* fusion

317   gene was generated in both wild-type and DM *ERG11* strains. Appropriate transformants were

318   placed on media lacking (SC) or containing excess methionine (SC+methionine) and allowed to

319   grow. Two independent isolates of each *MET3-UPC2A* transformant were tested to evaluate

320   strain variability in these assays.

321   Addition of methionine to strains containing the *MET3-UPC2A* fusion gene in addition to

322   the DM *ERG11* allele caused the growth of this strain to be further reduced when compared to

13

323   the presence of the wild-type *UPC2A* gene (Figure 7A, right hand panel). This result suggests

324   that reduction of Upc2A levels (by repression of the *MET3* promoter with methionine) caused a

325   growth defect in the presence of the DM *ERG11* mutation. When these *UPC2A* and *MET3-*

326   *UPC2A* strains containing the DM *ERG11* mutation were grown in the absence of exogenous

327   methionine, their growth was similar (Figure 7A left hand panel).

328   To determine the levels of Upc2A protein in these different strains, we prepared whole

329   cell protein extracts from these strains. These extracts were analyzed by western blotting using

330   the anti-Upc2A antiserum. The *MET3* promoter activity is highest in SC medium (29) and we

331   will consider the data from these media conditions first (Figure 7B, left hand panel). The *MET3*

332   promoter drove much higher levels of Upc2A protein than were produced from the native

333   *UPC2A* promoter in the presence of wild-type *ERG11* (compare lanes 1 and 3). The elevated

334   expression of Upc2A seen in wild-type cells containing *MET3-UPC2A* did not lead to a

335   corresponding increase in Erg11 expression (lanes 1 and 3). Interestingly, Upc2A levels were

336   dramatically reduced when the *MET3-UPC2A* fusion gene was present in the DM *ERG11* strain,

337   albeit to levels similar to those seen when Upc2A was produced by the native *UPC2A* gene

338   (compare lanes 2 and 4). The presence of the *MET3-UPC2A* allele did not affect the observed

339   induction of Erg11 in the presence of the DM *ERG11* allele (compare lanes 2 and 4), potentially

340   due to the surprisingly low levels of Upc2A driven by the *MET3-UPC2A* allele when the DM

341   *ERG11* mutant was present. The lack of any detectable Upc2A expression differences in the

342   two DM *ERG11* strains (varying due to their different *UPC2A* promoters) also correlated well

343   with the equivalent ability of these strains to grow on SC medium (Figure 7A above).

344   When methionine was added to repress *MET3-UPC2A* transcription, the levels of the

345   corresponding Upc2A protein were strongly reduced as expected (Figure 7B, right hand panel).

346   However, the reduction of Upc2A upon methionine repression led to different levels of this

347   transcription factor in a manner dependent on the *ERG11* allele present in the cell. Methionine

348   repression of the *MET3-UPC2A* in the DM *ERG11* strain blocked the production of a detectable

14

349   level of Upc2A while this same treatment of cells carrying wild-type *ERG11* still produced readily

350   detectable Upc2A (compare lanes 7 and 8). The extremely low level Upc2A production seen in

351   the methionine-repressed *MET3-UPC2A* with DM *ERG11* may explain the methionine-

352   dependent growth defect seen in this strain (see Figure 7A). These low levels of Upc2A also

353   blocked the normal increase in Erg11 and Pdr1 caused by the DM *ERG11* allele (compare lanes

354   6 and 8), suggesting that both Erg11 and Pdr1 expression were, in part, driven by Upc2A

355   function in this mutant background.

356   We carried out this same analysis but using a *MET3-PDR1* gene (Supplemental Figure

357   2). In the absence of fluconazole, there was no significant effect of the *MET3-PDR1* fusion

358   gene on growth of either the wild-type or DM *ERG11* strain irrespective of the presence of

359   methionine (Supplemental Figure 2A). The addition of fluconazole revealed the strong increase

360   in resistance shown by the DM *ERG11* strains in the presence of either the wild-type or *MET3-*

361   driven *PDR1* gene, in the absence of methionine (Supplemental Figure 2A, top panels). The

362   addition of methionine to these media to repress *MET3-PDR1* (Supplemental Figure 2A, bottom

363   panels) caused a loss of fluconazole resistance at the highest concentration tested. These data

364   illustrate the critical contribution made by Pdr1 to the fluconazole resistance phenotype of the

365   DM *ERG11* strain.

366   Western blot analyses were carried out to determine the effect of the *MET3-PDR1* gene

367   on expression of Pdr1 itself, Cdr1 and Erg11 (Supplemental Figure 2B). Steady-state levels of

368   Pdr1 were much higher in the presence of the wild-type *ERG11* gene than in the DM *ERG11-*

369   containing strain (compare lanes 1 and 3). The expression of Pdr1 in these two strains was

370   inversely correlated with expression of the Pdr1 target gene *CDR1* as evidenced by the high

371   Cdr1 levels in the DM *ERG11* strain compared to the wild-type strain (compare lanes 1 and 3).

372   This finding suggests that Pdr1 is activated in the presence of the DM *ERG11* allele as its

373   steady-state expression is lower yet Cdr1 expression is higher. Previously, we used the *MET3*

374   promoter to produce either wild-type or GOF Pdr1 proteins (30). The GOF proteins were found

15

375   to be less stable than the corresponding wild-type factor. Production of this hypomorphic form

376   of Erg11, in the absence of any azole drug, was sufficient to strongly induce Pdr1 activity and

377   Cdr1 synthesis.

378

379   Discussion

380

381   One of the nearly inevitable outcomes from the extensive use of fluconazole as an

382   antifungal drug has been the development of resistance. Mutant forms of *ERG11* have been

383   found in every *Candida* species with the exception of *C. glabrata* and *C. krusei* (31). Detailed

384   analyses of the *C. albicans* Erg11 enzyme have clearly implicated structural changes within

385   azole-resistant mutant forms of this enzyme leading to reduced azole susceptibility (reviewed in

386   (32)). Azole resistance caused by mutational alteration within Erg11 is most parsimoniously

387   interpreted in this manner.

388   Our data provide a second means of *ERG11* mutants impacting azole resistance via a

389   secondary effect on expression of Pdr1/*CDR1* in *C. glabrata*. While it is clear that the mutants

390   we have characterized here have effects in addition to activation of Pdr1, genetic depletion of

391   Pdr1 caused an approximate 5-fold reduction in fluconazole resistance in the DM *ERG11* strain

392   (Supplemental Figure 2). This type of a secondary effect can have major implications in the

393   observed azole resistance of a given *ERG11* mutant background and is an important

394   consideration in evaluation of this phenotype.

395   Fluconazole resistant clinical isolates of *C. albicans* are readily recovered with lesions in

396   the Ca*ERG11* gene but azole resistant isolates with mutations in this locus have rarely been

397   reported in *C. glabrata* (33). We constructed *C. glabrata ERG11* mutations based on cognate

398   changes in the *C. albicans* gene. We selected positions Y141 and S410 in the *C. glabrata*

399   enzyme as the analogous positions in the *C. albicans* Erg11 could be found mutated either

400   alone or together in azole-resistant clinical isolates (9). The *C. glabrata* equivalent mutations

16

401   caused azole resistance as expected but the DM allele also exhibited a growth defect, even on

402   rich YPD medium, which was not reported for the *C. albicans* mutant. This growth defect, at

403   least for the DM *ERG11* mutant, may be part of the reason that mutations in *ERG11* are not

404   found in *C. glabrata* isolates. Confirmation of this suggestion will require more detailed study of

405   the corresponding mutations in *C. albicans* as well as analyses of additional *ERG11* mutants in

406   *C. glabrata.*

407   The DM *ERG11* allele was also found to cause several other drug phenotypes. The

408   increased resistance to caspofungin was not expected and may involve induction of the *FKS2*

409   gene (Figure 2D). We have preliminary evidence that Upc2A may act to control expression of

410   β-glucan synthase (20) but have not yet linked this to *FKS2*. Crz1 is a well-established

411   transcriptional activator of *FKS* gene expression (34, 35) and we provide evidence that the

412   CRZ1 gene must be intact for the DM *ERG11* allele to induce caspofungin resistance (Figure

413   2E).

414   The DM *ERG11* seems to be acting as a reduced function or hypomorphic allele of this

415   gene. This was evidenced by the reduced level of ergosterol accumulation in the DM mutant

416   background and the increased amphotericin B resistance. We suggest that this reduction in

417   function is critical for the observed induction of the *ERG* pathway genes as well as the

418   Pdr1/*CDR1* regulatory circuit. Previous work from our lab showed that genetically depleting

419   Erg11 by repression of two different artificial promoters driving *ERG11* caused the same

420   changes in gene regulation (19). The behavior of the DM *ERG11* mutant strain provides further

421   support for our hypothesis that a physiological link exists between the ergosterol biosynthetic

422   pathway and Pdr1 (18).

423   Comparison of the DM *ERG11* allele with each of the two single mutant alleles suggests

424   that there is a synthetic interaction between the Y141H and S410F mutations. In neither of the

425   two single mutants was evidence obtained that endogenous downstream gene expression was

426   being induced in the presence of these altered enzymes. However, when both of these lesions

427   were present in the same protein, a range of downstream responses were triggered. These

428   include *FKS2* induction and Pdr1 activation along with Upc2A. This was not observed with the

429   single mutants. We suggest that the single mutants seem to cause increased fluconazole

430   resistance primarily through their action on activity of the altered enzyme. The very sensitive 5X

431   SRE-*CYC1-lacZ* reporter plasmid was modestly induced in the presence of each single mutant

432   Erg11 (Figure 4B) but their effect was small compared to the induction caused by the DM Erg11

433   protein. The combination of the two single mutations led to production of a more defective

434   Erg11 protein that in turn caused intracellular responses such as activation of Upc2A and Pdr1.

435   The activation of Upc2A-dependent transcription is a central feature of the cellular

436   response to the presence of the DM *ERG11* allele. We produced a conditional *MET3-UPC2A*

437   strain that contained the DM *ERG11* mutation to avoid any problematic interactions caused by

438   introduction of a *upc2AΔ* null allele into this strain. The essential contribution of Upc2A to the

439   maintenance of the DM *ERG11*-containing strain could be shown by the severe growth defect

440   caused by methionine repression of this *UPC2A* allele (Figure 7A). We suggest that the

441   presence of the DM *ERG11* allele led to induction of Upc2A function which in turn is linked to an

442   increased level of degradation of this active transcription factor. This suggestion is supported

443   by the inhibition of *MET3-UPC2A* transcription by the addition of methionine leading to a drop in

444   Upc2A levels below the limit of detection in the DM *ERG11* background (Figure 7B). This is

445   roughly the equivalent of a direct protein stability assay as we block synthesis at the level of

446   transcription while allowing degradation to proceed without intervention. The apparent instability

447   of the wild-type Upc2A after activation by the presence of the DM Erg11 protein is very similar to

448   the instability found when GOF forms of Pdr1 are compared to wild-type Pdr1 (17) . These

449   factors are evidently deleterious for the cell to maintain in their activated states unless their

450   presence is crucial for a given stress response. We have previously observed this as a

451   hyperactive mutant form of Pdr1 can be lethal (17). These data suggest that an important

452   control point for Upc2A may lie at the level of protein stability.

18

453   One reason for constructing these different fluconazole resistant forms of Erg11 in *C.*

454 *glabrata* was to see if their presence would influence fluconazole induction of Pdr1. It is

455 possible that fluconazole resistant forms of Erg11 would no longer respond to challenge by this

456 azole drug. However, that was not the case as all strains expressing fluconazole resistant

457 *ERG11* allele still showed induction of the Pdr1/*CDR1* regulatory axis upon fluconazole

458 exposure (Figure 3). The striking induction of *CDR1*, *PDR1* and *ERG11* expression when the

459 DM *ERG11* allele is present with no fluconazole addition argues that these genes and the

460 pathways they define are normally co-regulated, irrespective of the presence of drug.

461   The simplest interpretation for azole resistant *ERG11* mutations in multiple organisms

462 has been that the altered enzymes may no longer be able to interact with azole drugs and this

463 can explain their resistance phenotype. While this is certainly true for some mutants (such as

464 the two single mutant alleles of *ERG11* analyzed here), there are likely to be more complex

465 physiological responses to these mutant enzymes that can alter the resistance phenotype in

466 *ERG11* mutant strains. Ergosterol is an essential constituent of the fungal cell membrane and

467 limiting its biosynthesis triggers transcriptional correction in most fungi examined (5, 36, 37). In

468 *C. glabrata*, there appears to be a threshold of ergosterol limitation that is not crossed by the

469 single mutant forms of Erg11 but is exceeded by the DM Erg11 enzyme. Exceeding this

470 threshold leads to activation of downstream pathways to deal with the detected ergosterol

471 limitation.

472   Our finding of these deeper regulatory connections between ergosterol biosynthesis and

473 transcription circuitry including but not restricted to factors directly involved in *ERG* gene control

474 suggests that additional linkages of this type may be participating in azole resistance in other

475 fungi. Azole-resistant forms of *Aspergillus fumigatus* are commonly associated with substitution

476 mutations within the *cyp51A* gene (*ERG11* equivalent in *Aspergilli*) (37). Some of the most

477 common azole-resistant alleles found in *A. fumigatus* are the result of linked changes in which a

478 residue in the coding sequence is changed and a region of the promoter is duplicated

479   (Reviewed in (38)). These linked changes act together to enhance azole resistance more than

480   either alone (39), suggesting that alleles of this sort engage more than one mechanism to affect

481   azole resistance. We have previously shown that the L98H form of Cyp51A in *A. fumigatus*

482   produces lower levels of this enzyme than the wild-type yet is still resistant to voriconazole (40).

483   Additionally, mutations in the HMGCoA reductase gene (*hmg1*) from *A. fumigatus* also causes a

484   strong decrease in voriconazole susceptibility although *cyp51A* gene expression appeared to be

485   unaffected (41). These observations suggest that other fungi may also employ additional

486   transcriptional circuitry to impact azole resistance in response to alterations in ergosterol

487   biosynthesis. Identifying and characterizing these other transcriptional contributors to azole

488   resistance are important goals in the dissection of the molecular basis of azole resistance.

489

490   Materials and Methods

491

492   Strains and growth conditions.

493   *C. glabrata* was grown in rich YPD medium (1% yeast extract, 2% peptone, 2% glucose) or

494   under amino acid-selective conditions in complete supplemental medium (CSM) (Difco yeast

495   nitrogen extract without amino acids, amino acid powder from Sunrise Science Products, 2%

496   glucose). YPD media supplemented with 50 µg/ml nourseothricin (Jena Bioscience, Jena,

497   Germany) and 2 mM methionine was used to select strains containing pBV65 vector derivatives

498   (42). CSM media (2% glucose, 1mM estradiol) without methionine was used to recycle the

499   selection cassette on pBV65. YPD solid agar supplemented with 1 mg/ml 5-fluoro-orotic acid

500   was used to cure the pBV43 plasmid. All strains used in this study are listed in Table 1.

501

502   Plasmid construction and promoter mutagenesis.

503   All constructs used for homologous recombination into the chromosome were constructed in the

504   pUC19 vector (New England Biolabs, Ipswich, MA). PCR was used to amplify DNA fragments.

20

505   PCR products were run on 1.5 % agarose gel (RPI, Troy, NY), excised and purified with

506   Purelink quick gel extraction and PCR cleaning combo kit (Invitrogen, Carlsbad, CA). Gibson

507   assembly cloning (New England Biolabs) was routinely used to assemble fragments together

508   into appropriate plasmid backbones. All isogenic deletion constructs were made by assembling

509   the recyclable cassette from pBV65 and fragments from the immediate upstream and

510   downstream regions of the target genes. Fragments of the target genes were amplified from

511   CBS138 background. Eviction of the recyclable cassette left a single copy of *loxP* in place of the

512   excised target gene coding region.

513   *PDR1* constructs were made by using Gibson assembly (43) to produce fragments

514   corresponding to the wild-type, R376W or D1082G alleles of *PDR1* with a recyclable cassette

515   located downstream from the natural stop codon. Eviction of the recyclable cassette in the

516   integrated constructs left a single copy of *loxP* 250-300 base-pairs downstream of the target

517   gene stop codons. R376W and D1082G forms of *PDR1* were amplified from pSK70 and pSK71

518   backgrounds (17).

519   *ERG11* wild-type and mutant integration constructs were made as above with the

520   resulting fragments corresponding to the wild-type, Y141H, S410F or the Y141H S410F alleles

521   of *ERG11* with the *his3MX6* (19) marker located 270 bp from the natural stop codon.

522   Conversion of strains to *LEU2* was done by PCR amplifying the *LEU2* coding region

523   along with 500 base pairs immediately upstream and downstream from the CBS138

524   background. Linear DNA was then transformed into KKY2001 and the colonies were selected

525   on CSM agar without leucine.

526   To generate the *S. cerevisiae ERG11* complementing plasmid (pBV43), the Sc*ERG11*

527   promoter (800 bps upstream of AUG), Sc*ERG11* coding sequence, and Sc*ERG11* terminator

528   (350 bps downstream of the stop codon) were PCR amplified from the an S288c wild-type strain

529   (SEY6210). This fragment was then cloned into the pCU-MET3 vector (29), which was pre-

530   digested with SacI and XhoI.

21

531   The Sterol Response Element (SRE) reporter construct (pBV382) was produced by

532   cloning the E. coli *lacZ* gene as a PCR fragment from pSK80 (17). This fragment was then

533   cloned into the pCL vector (29), which was pre-digested with SalII and XhoI. A Upc2A-

534   responsive promoter cassette, containing the 5 concatemerized copies of the *ERG1* promoter

535   SRE (-725 to -775) located downstream from the *ADH1* terminator and upstream of the *CYC1*

536   minimal promoter, was generated by Genscript (Piscataway, NJ). The Upc2A responsive

537   promoter was PCR amplified and cloned into the pCL-*lacZ* vector, digested with SacI and SalI.

538   The control vector (pBV378) was constructed by cloning the *ADH1* terminator and the *CYC1*

539   minimal promoter, PCR amplified from BVGC7 (19), into the pCL-*lacZ* vector, digested with SacI

540   and SalI.

541   To generate the *MET3*-driven *UPC2A* and *PDR1* strains, the *MET3* promoter and the

542   *URA3* gene were PCR amplified from the pUC-*MET3* plasmid. This *URA3-MET3* promoter

543   cassette was placed immediately upstream of the target gene AUG codon by recombination into

544   the gene of interest.

545

546   *C. glabrata* transformation.

547   Cell transformations were performed using a lithium acetate method. After being heat shocked,

548   cells were either directly plated onto selective CSM agar plates (for auxotrophic

549   complementation) or grown at 30°C at 200 rpm overnight (for nourseothricin selection).

550   Overnight cultures were then plated on YPD agar plates supplemented with 50 µg/ml of

551   nourseothricin. Plates were incubated at 30°C for 24 to 48 hours. In case of chromosomal

552   insertion, individual colonies were isolated and screened by PCR for correct insertion of the

553   targeted construct.

554

555   Construction of mutant *ERG11* strains

22

556   Since Erg11 is essential for *C. glabrata* aerobic growth (44) ,A *URA3* (*ScURA3*)-containing

557   plasmid shuffling technique was used to construct *ERG11* mutant alleles in the SPG96 (*ura3Δ*)

558   *C. glabrata* strain (17). An autonomous plasmid pBV43 marked with *ScURA3* and containing the

559   wild-type Sc*ERG11* was first transformed into the SPG96 strain. Then *ERG11* was deleted in

560   the chromosome by homologous recombination, leaving Sc*ERG11* on pBV43 functioning as the

561   sole copy of the *ERG11* gene. Next, the wildtype *C. glabrata ERG11* and the 3 mutant alleles

562   were individually reintroduced to the normal locus by homologous recombination with selection

563   for His+ transformants. Finally, the pBV43 plasmid was cured with 1 mg/ml 5-FOA on a YPD

564   agar plate to construct the *C. glabrata* strains, BVGC344 (*ERG11*), BVGC346 (Y141H *ERG11*),

565   BVGC336 (S410F *ERG11*), and a strain containing an ERG11 gene with both of these

566   mutations present (BVGC340: DM *ERG11*).

567

568   Total sterol estimation.

569   Cell total sterol was extracted and measured as previously described (19). In short, cell pellets

570   were lysed in 25% alcoholic potassium hydroxide at 90°C for 2 hours. Total sterol was

571   detected by spectrophotometric scanning between the wavelengths of 240 nm and 300nm.

572   The presence of ergosterol in the extracted sample resulted in a four-peak curve with peaks

573   located at approximately 262, 270, 281, and 290 nm.

574

575   Quantification of transcript levels by RT-qPCR.

576   Total RNA was extracted from cells by extraction using TRIzol (Invitrogen) and chloroform

577   (Fisher Scientific, Hampton, NH) followed by purification with RNeasy minicolumns (Qiagen,

578   Redwood City, CA). 500 ng -1 μg total RNA was reverse-transcribed using an iScript cDNA

579   synthesis kit (Bio-Rad, Des Plaines, IL). Assay of RNA via quantitative PCR (qPCR) was

580   performed with iTaq universal SYBR green supermix (Bio-Rad). Target gene transcript levels

581   were normalized to transcript levels of 18S rRNA.

582

583   Spot test assay.

584   Cells were grown in YPD medium to mid-log-phase. Cultures were then 10-fold serially diluted

585   and spotted onto YPD agar plates containing different concentrations of fluconazole (LKT

586   laboratories, St Paul, MN), caspofungin (Apexbio, Houston, TX) or Amphotericin B (Sigma). All

587   agar plates were incubated at 30°C for 24 to 48 h before imaging was performed.

588

589   β-galactosidase assay.

590   Harvested cells were lysed with glass beads (Scientific Industries Inc) in breaking buffer (100

591   mM Tris pH8, 1 mM Dithiothreitol, and 20% Glycerol) at 4^oC for 10 min. Lysate was collected

592   and β-galactosidase enzymatic reaction was carried out in Z-buffer (60 mM Na_2HPO_4, 40 mM

593   NaH_2PO_4, 10 mM KCl, 1 mM $MgSO_4$, 50 mM 2-Mercaptoethanol) with 650 μg/ml O-nitrophenyl-

594   β-D-galactopyranoside (ONPG). Miller units were calculated based on the equation: (OD_{420} x

595   1.7) / (0.0045 x total protein concentration x used extract volume x time). Bradford assay (Bio-

596   Rad) was used to measure the total protein concentration in the lysate.

597

598   Chromatin immunoprecipitation (ChIP).

599   The detailed ChIP protocol was previously described (19). The sheared chromatin was

600   incubated with rabbit polyclonal anti-Upc2A antibody (1:50 dilution) or rabbit IgG control

601   antibody, NBP2-24891 (Novus Biologicals, Centennial, CO) for 2 h before being incubated

602   together with 30 μl of washed protein G Dynabeads (Life Technologies) overnight on a nutator

603   at $4^°$ C. Washing, reversal of cross-links, and purification of DNA processed by the use of ChIP

604   were performed as described in (19).

605

606   Real-time PCR was performed on ChIP purified DNA, under the following conditions: 1 cycle of

607   95°C for 30 s followed by 40 cycles of 95°C for 15 s and 57°C for 30 s on a MyiQ2 Bio-Rad

24

608   machine. A 1 µl volume of the DNA processed by the use of ChIP (diluted 5-fold) or of input

609   (diluted 20-fold) DNA was used in a reaction mixture with a 20 µl total volume using SYBR

610   green master mix (Bio-Rad) and a 0.4 µM concentration of each primer. The percent input

611   method was used to calculate the signal of enrichment of the promoter region for each gene.

612   *ERG11*, *CDR1*, and *PDR1* promoters were analyzed with primers specifically targeting the

613   *ERG11* promoter (−561 to −694 relative to the ATG as +1), *CDR1* promoter (−476 to −665), and

614   *PDR1* promoter (−551 to −651) regions. A region of *ERG11*, located within the coding sequence

615   (+939 to +1042) and the *HO* promoter (-585 to -751) region were used as negative controls.

616

617   Competitive growth assay.

618   The *LEU2* coding region along with its immediate 500 bps up- and downstream sequences were

619   amplified from CBS138 genomic DNA. The product was then used to transform the *leu2Δ*::FRT

620   allele to *LEU2* in DM *ERG11* background at the *LEU2* native locus to generate BVGC365 (DM

621   *ERG11*/*LEU2*). A mid-log growth culture [between O.D. of 1 and 2] was diluted to 0.2 O.D. in

622   fresh YPD. Each culture to be tested: wild-type, R376W *PDR1* or D1082G *PDR1*, was mixed at

623   a 1:1 ratio with DM *ERG11*/*LEU2*, and the mixed cultures were treated either with fluconazole

624   (20 µg/ml) or ethanol for 24 hours at 30°C. Cultures were collected, serially diluted, and plated

625   on YPD and CSM media without leucine for colony forming unit analysis.

626

627   Antibodies and western immunoblotting.

628   Cells were lysed with lysis buffer (1.85 M NaOH, 7.5% 2-Mercaptoethanol). Proteins were

629   precipitated with 50% Trichloroacetic acid and resuspended in Urea buffer (40 mM Tris pH8, 8.0

630   M Urea, 5% SDS, 1% 2-Mercaptoethanol). Cdr1, Pdr1, and Upc2A rabbit polyclonal antibodies

631   were previously described (19). Anti-HA monoclonal antibody was purchased from Invitrogen.

632   Secondary antibodies were purchased from LI-COR Biosciences. Imaging was performed with

633   Odyssey CLx Imaging System (LI-COR Biosciences) and analyzed by Image Studio Lite

634   Software (LI-COR Biosciences). Detected target band fluorescence intensity was normalized

635   against tubulin fluorescence intensity and compiled from two biological replicate experiments

636   and two technical replicates in each experiment, giving four replicates in total. Erg11 anti-

637   peptide rabbit polyclonal antibody was produced by GenScript (Piscataway, NJ). The peptide

638   sequence was AKIYWEKRHPEQKY, and it covered the 520th to 533rd amino-acids in the

639   Erg11 protein primary sequence. The peptide antibody was confirmed by western blotting

640   comparing wild-type and a strain carrying an *ERG11*-3X HA allele. Anti-peptide antibody

641   detected native Erg11 from wild-type cells and the increased molecular mass of the Erg11-3X

642   HA protein. Dual color LI-COR secondary antibodies were used to overlap the band intensity of

643   Erg11 protein detected with anti-HA mouse monoclonal antibody and Erg11 peptide rabbit

644   polyclonal antibody

645

646   Statistics.

647   The Student T-test was used to assess the statistical significance of results of comparisons of

648   samples. Paired conditions were used for comparisons of results from the same isolate obtained

649   under different treatment conditions, while unpaired conditions were used for comparisons of

650   results from isolates obtained under the same treatment conditions (*, $P < 0.5$; **, $P < 0.01$; ***,

651     $P < 0.001$).

652

653   Acknowledgements

656

657   References

658

659

660   1.   Rodrigues ML. 2018. The Multifunctional Fungal Ergosterol. mBio 9.

661   2.   Sokolov SS, Trushina NI, Severin FF, Knorre DA. 2019. Ergosterol Turnover in Yeast:

662   An Interplay between Biosynthesis and Transport. Biochemistry (Mosc) 84:346-357.

663   3.   Zhang J, Li L, Lv Q, Yan L, Wang Y, Jiang Y. 2019. The Fungal CYP51s: Their

664   Functions, Structures, Related Drug Resistance, and Inhibitors. Front Microbiol 10:691.

665   4.   Warrilow AG, Martel CM, Parker JE, Melo N, Lamb DC, Nes WD, Kelly DE, Kelly SL.

666   2010. Azole binding properties of Candida albicans sterol 14-alpha demethylase (CaCYP51).

667   Antimicrob Agents Chemother 54:4235-45.

668   5.   Jorda T, Puig S. 2020. Regulation of Ergosterol Biosynthesis in Saccharomyces

669   cerevisiae. Genes (Basel) 11.

670   6.   Keniya MV, Sabherwal M, Wilson RK, Woods MA, Sagatova AA, Tyndall JDA, Monk BC.

671   2018. Crystal Structures of Full-Length Lanosterol 14alpha-Demethylases of Prominent Fungal

672   Pathogens Candida albicans and Candida glabrata Provide Tools for Antifungal Discovery.

673   Antimicrob Agents Chemother 62.

674   7.   Sagatova AA, Keniya MV, Wilson RK, Monk BC, Tyndall JD. 2015. Structural Insights

675   into Binding of the Antifungal Drug Fluconazole to Saccharomyces cerevisiae Lanosterol

676   14alpha-Demethylase. Antimicrob Agents Chemother 59:4982-9.

677   8.   Warrilow AG, Parker JE, Kelly DE, Kelly SL. 2013. Azole affinity of sterol 14alpha-

678   demethylase (CYP51) enzymes from Candida albicans and Homo sapiens. Antimicrob Agents

679   Chemother 57:1352-60.

680   9.   Sanglard D, Ischer F, Koymans L, Bille J. 1998. Amino acid substitutions in the

681   cytochrome P-450 lanosterol 14alpha-demethylase (CYP51A1) from azole-resistant Candida

682   albicans clinical isolates contribute to resistance to azole antifungal agents. Antimicrob Agents

683   Chemother 42:241-53.

684   10.   Flowers SA, Colon B, Whaley SG, Schuler MA, Rogers PD. 2015. Contribution of

685   clinically derived mutations in ERG11 to azole resistance in Candida albicans. Antimicrob

686   Agents Chemother 59:450-60.

687   11.   Kelly SL, Lamb DC, Kelly DE. 1999. Y132H substitution in Candida albicans sterol

688   14alpha-demethylase confers fluconazole resistance by preventing binding to haem. FEMS

689   Microbiol Lett 180:171-5.

690   12.   Kelly SL, Lamb DC, Loeffler J, Einsele H, Kelly DE. 1999. The G464S amino acid

691   substitution in Candida albicans sterol 14alpha-demethylase causes fluconazole resistance in

692   the clinic through reduced affinity. Biochem Biophys Res Commun 262:174-9.

693   13.   Warrilow AG, Mullins JG, Hull CM, Parker JE, Lamb DC, Kelly DE, Kelly SL. 2012. S279

694   point mutations in Candida albicans Sterol 14-alpha demethylase (CYP51) reduce in vitro

695   inhibition by fluconazole. Antimicrob Agents Chemother 56:2099-107.

696   14.   Marichal P, Koymans L, Willemsens S, Bellens D, Verhasselt P, Luyten W, Borgers M,

697   Ramaekers FCS, Odds FC, Vanden Bossche H. 1999. Contribution of mutations in the

698   cytochrome P450 14alpha-demethylase (Erg11p, Cyp51p) to azole resistance in Candida

699   albicans. Microbiology (Reading) 145 (Pt 10):2701-2713.

700   15.   Warrilow AG, Nishimoto AT, Parker JE, Price CL, Flowers SA, Kelly DE, Rogers PD,

701   Kelly SL. 2019. The Evolution of Azole Resistance in Candida albicans Sterol 14alpha-

702   Demethylase (CYP51) through Incremental Amino Acid Substitutions. Antimicrob Agents

703   Chemother 63.

704   16.   Moye-Rowley WS. 2019. Multiple interfaces control activity of the Candida glabrata Pdr1

705   transcription factor mediating azole drug resistance. Curr Genet 65:103-108.

706   17.   Khakhina S, Simonicova L, Moye-Rowley WS. 2018. Positive autoregulation and

707   repression of transactivation are key regulatory features of the Candida glabrata Pdr1

708   transcription factor. Mol Microbiol 107:747-764.

709   18.   Moye-Rowley WS. 2020. Linkage between genes involved in azole resistance and

710   ergosterol biosynthesis. PLoS Pathog 16:e1008819.

711   19.   Vu BG, Thomas GH, Moye-Rowley WS. 2019. Evidence that Ergosterol Biosynthesis

712   Modulates Activity of the Pdr1 Transcription Factor in Candida glabrata. MBio 10.

713   20.   Vu BG, Stamnes MA, Li Y, Rogers PD, Moye-Rowley WS. 2021. Azole resistance is

714   mediated by integration of sterol gene regulation and membrane transporter production by the

715   zinc cluster-containing transcription factor Upc2A in Candida glabrata. bioRxiv

716   doi:10.1101/2021.05.07.443069:2021.05.07.443069.

717   21.   Monk BC, Tomasiak TM, Keniya MV, Huschmann FU, Tyndall JD, O'Connell JD, 3rd,

718   Cannon RD, McDonald JG, Rodriguez A, Finer-Moore JS, Stroud RM. 2014. Architecture of a

719   single membrane spanning cytochrome P450 suggests constraints that orient the catalytic

720   domain relative to a bilayer. Proc Natl Acad Sci U S A 111:3865-70.

721   22.   Xiang MJ, Liu JY, Ni PH, Wang S, Shi C, Wei B, Ni YX, Ge HL. 2013. Erg11 mutations

722   associated with azole resistance in clinical isolates of Candida albicans. FEMS Yeast Res

723   13:386-93.

724   23.   Davies BS, Wang HS, Rine J. 2005. Dual activators of the sterol biosynthetic pathway of

725   Saccharomyces cerevisiae: similar activation/regulatory domains but different response

726   mechanisms. Mol Cell Biol 25:7375-85.

727   24.   Marie C, Leyde S, White TC. 2008. Cytoplasmic localization of sterol transcription

728   factors Upc2p and Ecm22p in S. cerevisiae. Fungal Genet Biol 45:1430-8.

729   25.   Yang H, Tong J, Lee CW, Ha S, Eom SH, Im YJ. 2015. Structural mechanism of

730   ergosterol regulation by fungal sterol transcription factor Upc2. Nat Commun 6:6129.

731   26.   Vermitsky JP, Edlind TD. 2004. Azole resistance in Candida glabrata: coordinate

732   upregulation of multidrug transporters and evidence for a Pdr1-like transcription factor.

733   Antimicrob Agents Chemother 48:3773-81.

734   27.   Tsai HF, Krol AA, Sarti KE, Bennett JE. 2006. Candida glabrata PDR1, a transcriptional

735   regulator of a pleiotropic drug resistance network, mediates azole resistance in clinical isolates

736   and petite mutants. Antimicrob Agents Chemother 50:1384-92.

737   28.   Ferrari S, Ischer F, Calabrese D, Posteraro B, Sanguinetti M, Fadda G, Rohde B,

738   Bauser C, Bader O, Sanglard D. 2009. Gain of function mutations in CgPDR1 of Candida

739   glabrata not only mediate antifungal resistance but also enhance virulence. PLoS Pathog

740   5:e1000268.

741   29.   Zordan RE, Ren Y, Pan SJ, Rotondo G, De Las Penas A, Iluore J, Cormack BP. 2013.

742   Expression plasmids for use in Candida glabrata. G3 (Bethesda) 3:1675-86.

743   30.   Simonicova L, Moye-Rowley WS. 2020. Functional information from clinically-derived

744   drug resistant forms of the Candida glabrata Pdr1 transcription factor. PLoS Genet

745   16:e1009005.

746   31.   Berkow EL, Lockhart SR. 2017. Fluconazole resistance in Candida species: a current

747   perspective. Infect Drug Resist 10:237-245.

748   32.   Parker JE, Warrilow AG, Price CL, Mullins JG, Kelly DE, Kelly SL. 2014. Resistance to

749   antifungals that target CYP51. J Chem Biol 7:143-61.

750   33.   Hull CM, Parker JE, Bader O, Weig M, Gross U, Warrilow AG, Kelly DE, Kelly SL. 2012.

751   Facultative sterol uptake in an ergosterol-deficient clinical isolate of Candida glabrata harboring

752   a missense mutation in ERG11 and exhibiting cross-resistance to azoles and amphotericin B.

753   Antimicrob Agents Chemother 56:4223-32.

754   34.   Matheos DP, Kingsbury TJ, Ahsan US, Cunningham KW. 1997. Tcn1p/Crz1p, a

755   calcineurin-dependent transcription factor that differentially regulates gene expression in

756   Saccharomyces cerevisiae. Genes Dev 11:3445-58.

757   35.   Stathopoulos AM, Cyert MS. 1997. Calcineurin acts through the CRZ1/TCN1-encoded

758   transcription factor to regulate gene expression in yeast. Genes Dev 11:3432-44.

30

759 36. Lv QZ, Yan L, Jiang YY. 2016. The synthesis, regulation, and functions of sterols in

760 Candida albicans: Well-known but still lots to learn. Virulence 7:649-59.

761 37. Dhingra S, Cramer RA. 2017. Regulation of Sterol Biosynthesis in the Human Fungal

762 Pathogen Aspergillus fumigatus: Opportunities for Therapeutic Development. Front Microbiol

763 8:92.

764 38. Chowdhary A, Kathuria S, Xu J, Meis JF. 2013. Emergence of azole-resistant aspergillus

765 fumigatus strains due to agricultural azole use creates an increasing threat to human health.

766 PLoS Pathog 9:e1003633.

767 39. Mellado E, Garcia-Effron G, Alcazar-Fuoli L, Melchers WJ, Verweij PE, Cuenca-Estrella

768 M, Rodriguez-Tudela JL. 2007. A new Aspergillus fumigatus resistance mechanism conferring

769 in vitro cross-resistance to azole antifungals involves a combination of cyp51A alterations.

770 Antimicrob Agents Chemother 51:1897-904.

771 40. Paul S, Diekema D, Moye-Rowley WS. 2017. Contributions of both ATP-Binding

772 Cassette Transporter and Cyp51A Proteins Are Essential for Azole Resistance in Aspergillus

773 fumigatus. Antimicrob Agents Chemother 61.

774 41. Rybak JM, Ge W, Wiederhold NP, Parker JE, Kelly SL, Rogers PD, Fortwendel JR.

775 2019. Mutations in hmg1, Challenging the Paradigm of Clinical Triazole Resistance in

776 Aspergillus fumigatus. mBio 10.

777 42. Vu BG, Moye-Rowley WS. 2018. Construction and Use of a Recyclable Marker To

778 Examine the Role of Major Facilitator Superfamily Protein Members in Candida glabrata Drug

779 Resistance Phenotypes. mSphere 3.

780 43. Gibson DG, Young L, Chuang RY, Venter JC, Hutchison CA, 3rd, Smith HO. 2009.

781 Enzymatic assembly of DNA molecules up to several hundred kilobases. Nat Methods 6:343-5.

782 44. Geber A, Hitchcock CA, Swartz JE, Pullen FS, Marsden KE, Kwon-Chung KJ, Bennett

783 JE. 1995. Deletion of the Candida glabrata ERG3 and ERG11 genes: effect on cell viability, cell

784   growth, sterol composition, and antifungal susceptibility. Antimicrob Agents Chemother 39:2708-

785   17.

786

787

788   Figure legends

789

790   Figure 1. **Construction of mutant *ERG11* alleles in *Candida glabrata*.** A. Amino acid

791   sequence comparison between Erg11 proteins from *Saccharomyces cerevisiae*, *Candida*

792   *glabrata* and *Candida albicans*. Graphic indication of amino acid identity between these three

793   yeast enzymes is shown with a red bar indicating 100%, while light and dark green denotes

794   66% or no conservation. Expanded regions with conserved residues are shown to illustrate the

795   positions that were mutated in *C. glabrata* to match changes associated with fluconazole

796   resistance originally found in *C. albicans*. B. Isogenic *C. glabrata* strains containing the

797   indicated *ERG11* alleles were grown to mid-log phase and plated as serial dilutions on rich

798   medium (YPD) or the same medium containing the indicated concentrations of antifungal drugs.

799   The strain containing both the Y141H- and S410F-encoding alleles was designated double

800   mutant (DM). Plates were allowed to develop at 30°C and then photographed. Antifungal drugs

801   are abbreviated as fluconazole (FLC), caspofungin (CSF) and amphotericin B (AmB).

802

803   Figure 2. **Ergosterol levels and caspofungin resistance-related mRNA production in**

804   ***ERG11* mutant strains.** Mid-log phase *C. glabrata* strains containing the indicated *ERG11*

805   alleles were either not treated (A) with fluconazole (20 µg/ml) (-FLC) or exposed to this drug for

806   3 (B) or 24 (C) hours. Total lipid extracts were prepared and analyzed for the levels of

807   ergosterol in each sample. D. Total RNA was extracted from isogenic wild-type and DM

808   *ERG11* strains without fluconazole treatment. Samples were then assayed for levels of the

809   indicated mRNAs using RT-qPCR. Relative expression level refers to the ratio of mRNA

810   produced in DM *ERG11* strains/wild-type strain. Baseline indicates equivalent expression in the

811   wildtype strain. E. Loss of *CRZ1* prevents increased caspofungin resistance of a DM *ERG11*

812   strain. The *CRZ1* gene was disrupted in wild-type and DM *ERG11* strains. These *crz1Δ*

813   derivatives and their isogenic wild-type strains were grown to mid-log phase and then analyzed

814   by serial dilution on YPD plates without (YPD) or containing the indicated levels of caspofungin.

815   Plates were incubated at 30°C for two days and photographed.

816

817   Figure 3. **Expression changes in response to *ERG11* alleles**. A. Levels of mRNA for *PDR1,*

818   *CDR1,* and *ERG11* were assayed by RT-qPCR in the indicated *ERG11* mutant strains during

819   growth in the absence (Control) or presence of fluconazole stress (Fluconazole). Fluconazole

820   treatment was 20 μg/ml for 2 hours. B. Whole cell protein extracts were prepared from the

821   same strains in A. These extracts were analyzed by western blotting using the indicated

822   antisera against Cdr1, Pdr1, Erg11, Upc2A or Tubulin. Equal loading and transfer of these

823   extracts was ensured by staining the nitrocellulose membrane with Ponceau S prior to antisera

824   incubation. C. Quantitation of 4 replicates of this western blotting is shown with the data

825   presented as the ratio of each strain relative to the wild-type cells. D. RT-qPCR analysis of

826   *ERG* gene expression in the DM *ERG11* mutant background relative to the wild-type level.

827   HMGCoA (HMG-CoA reductase) refers to the *HMG1* or *CAGL0L11506g* locus.

828

829   Figure 4. **Regulation of Upc2A in response to *ERG11* alleles**. A. Two different reporter

830   constructs carried on low-copy-number *C. glabrata* vectors that contained either the *S.*

831   *cerevisiae CYC1* promoter region with a translational fusion to *E. coli lacZ* (*CYC1-lacZ*) or the

832   same reporter construct with five copies of the *C. glabrata ERG1* sterol response element (SRE)

833   cloned upstream of the *CYC1* promoter (5X SRE-*CYC1-lacZ*) were introduced into the 3

834   different *C. glabrata* strains indicated at the top. These strains varied at their *UPC2A* allele

835   corresponding to a wild-type strain (*UPC2A*), gain-of-function form of *UPC2A* (G898D *UPC2A*)

836   or a null mutation (*upc2A∆*). Transformants were grown to mid-log phase and then assayed for

837   the level of β-galactosidase produced in each strain. B. The two different reporter plasmids

838   from A were introduced into the 4 isogenic *ERG11* mutant strains indicated. Transformants

839   were grown to mid-log phase and assayed for β-galactosidase levels. C. Chromatin

840   immunoprecipitation (ChIP) of Upc2A DNA-binding to genomic target sites. Total sheared and

841   crosslinked chromatin was prepared from either wild-type or DM *ERG11* cells. ChIP reactions

842   were carried out with either anti-Upc2A or a non-specific control antisera. Immunopurified DNA

843   was quantitated with qPCR using primer pairs that detected the promoters of *ERG11* (*ERG11*),

844   *CDR1* (*CDR1*), *PDR1* (*PDR1*) or *HO* (*HO*) along with a primer pair that detected a segment of

845   the *ERG11* coding sequence (*ERG11* cds). Data are plotted as the percentage of DNA

846   recovered in the immunopurified sample/total input DNA.

847

848   Figure 5. **Growth phenotypic comparison of DM *ERG11* with gain-of-function (GOF)**

849   **alleles of *PDR1*.** A. Isogenic mid-log phase *C. glabrata* strains containing *ERG11* wild-type or

850   DM alleles, *PDR1* null (*pdr1∆*), wild-type *PDR1* (*PDR1*::loxP), or two GOF alleles of *PDR1*

851   D1082G and R376W were serially diluted and spotted on YPD agar plates supplemented with

852   or without fluconazole (20 μg/ml). Plates were incubated at 30°C and photographed. B. Fitness

853   comparisons between the DM *ERG11* strain compared with wild-type (B), the GOF D1082G (C)

854   and R376W (D) *PDR1* mutant strains. Equal number of mid-log phase cells from each strain

855   were mixed together (Pretreatment). Cultures were then allowed to grow in the absence (YPD)

856   or presence of azole drug (Fluconazole) (20 μg/ml). At the end of incubation, samples of each

857   culture were plated and final distribution of each strain determined by plating. Deviations from

858   the starting 50:50 mix of strains would indicate a relative fitness advantage for one strain versus

859   the other.

34

860

861   Figure 6. **Relative gene expression responses to the DM *ERG11* or two different GOF**

862   ***PDR1* strains**. A. Strains varying at the *ERG11* or *PDR1* loci as indicated were grown in the

863   presence or absence of fluconazole as in Figure 3 and processed for RT-qPCR analyses of the

864   indicated mRNAs. B. The strains above were analyzed by western blotting as in Figure 3 using

865   antisera for Cdr1, Pdr1, Erg11, Upc2A or Tubulin (Tub). The membrane was stained after

866   transfer with Ponceau S as above. Quantitation of 4 western experiments is provided on the

867   right hand side of the figure.

868

869   Figure 7. **Depletion of Upc2A enhances growth defect of a DM *ERG11* strain**. A. The

870   *ERG11* promoter was replaced with the methionine-repressible *MET3* promoter in wild-type and

871   DM *ERG11* cells. Two different isolates of each *MET3* promoter replacement were grown to

872   mid-log phase, along with the isogenic wild-type and DM *ERG11* strains. These cells were

873   serially diluted onto plates containing either synthetic complete (SC) medium or the same

874   medium containing an excess of methionine (SC + methionine). Transformants were grown at

875   30°C and the plates photographed. B. The indicated strains were grown to mid-log phase in

876   the presence or absence of methionine and whole cell protein extracts prepared. These

877   extracts were analyzed as before using the indicated antisera. C. Quantitation of protein levels

878   in multiple western blots is shown. Significant changes are indicated with asterisks.

879

880   Supplemental Figure Legends

881

882   Supplemental Figure 1. **Voriconazole and itraconazole resistance among *ERG11***

883   **mutations**. Mid-log phase *C. glabrata* strains containing the indicated *ERG11* alleles were

884   serially diluted and spotted on YPD agar plates supplemented with various concentrations of

885   voriconazole (A) or itraconazole (B).

35

886

887   Supplemental Figure 2. **Interaction of DM *ERG11* allele and Pdr1.** A. The *PDR1* promoter

888   was replaced with the *MET3* promoter in strains containing either the wild-type or DM *ERG11*

889   allele. Strains were grown to mid-log phase and then serial dilutions plated on SC medium

890   lacking or containing methionine. Fluconazole was added to these plates where indicated.

891   Plates were incubated at 30°C and then photographed. B. The strains above were grown to

892   mid-log phase in SC medium lacking methionine, methionine was either omitted (-) or added (+)

893   and cultures allowed to continue to grow for equal times. Whole cell protein extracts were then

894   prepared and analyzed by western blotting using the indicated antibodies.

895
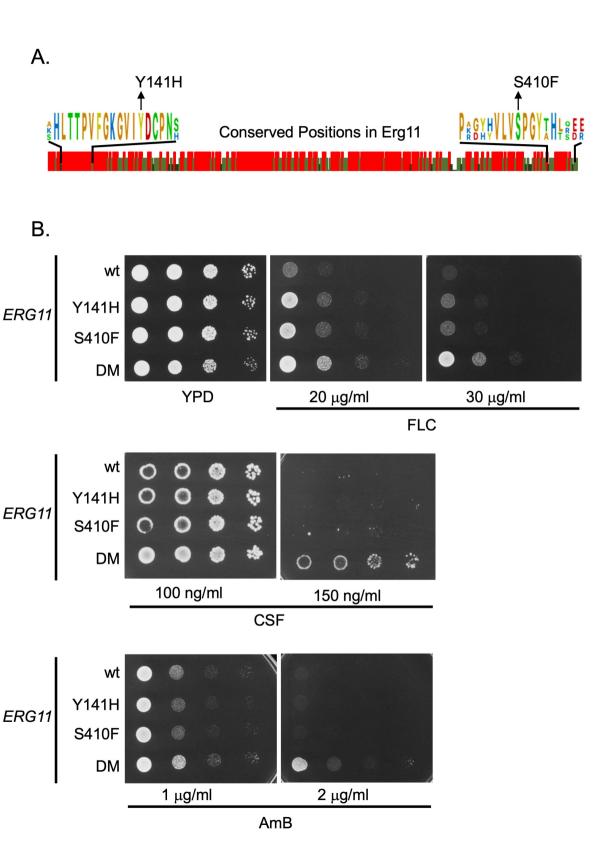
896

897

898

899

900   Table

Strain name	Parent	Genotype
SPG96	KKY2001	*his3Δ::FRT leu2Δ::FRT trp1Δ::FRT ura3Δ(-85+932)::Tn903NeoR*
BVGC14	SPG96	*his3Δ::FRT trp1Δ::FRT CEN-ScERG11/URA3 erg11Δ::LEU2*
BVGC344	BVGC14	*his3Δ::FRT leu2Δ::FRT trp1Δ::FRT ura3Δ(-85+932)::Tn903NeoR ERG11::HIS3*
BVGC346	BVGC14	*his3Δ::FRT leu2Δ::FRT trp1Δ::FRT ura3Δ(-85+932)::Tn903NeoR* Y141H *ERG11::HIS3*
BVGC336	BVGC14	*his3Δ::FRT leu2Δ::FRT trp1Δ::FRT ura3Δ(-85+932)::Tn903NeoR* S410F *ERG11::HIS3*
BVGC340	BVGC14	*his3Δ::FRT leu2Δ::FRT trp1Δ::FRT ura3Δ(-85+932)::Tn903NeoR* Y141H S410F *ERG11::HIS3*

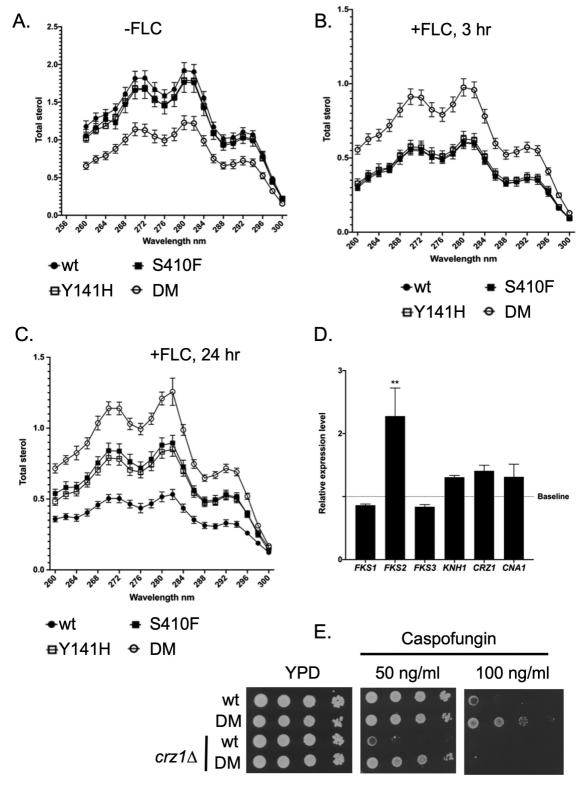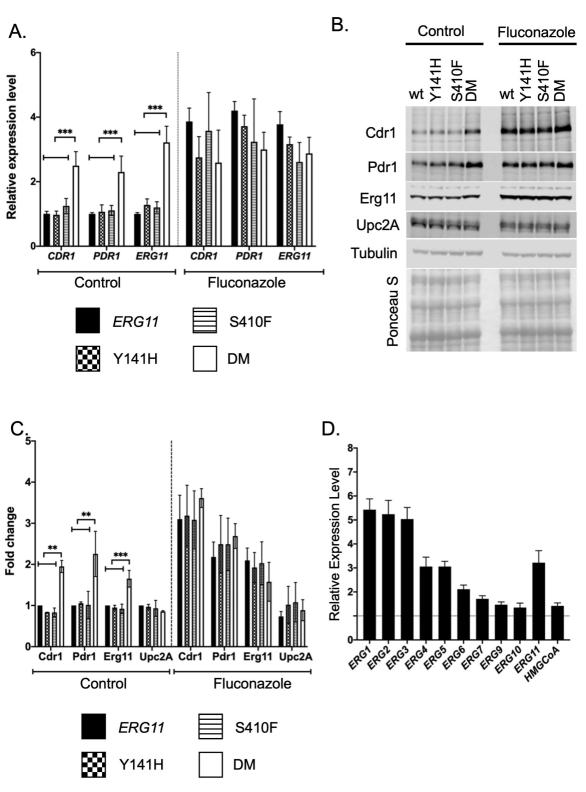| BVGC367	BVGC344	*his3Δ::FRT leu2Δ::FRT trp1Δ::FRT ura3Δ(-85+932)::Tn903NeoR ERG11::HIS3 pdr1Δ::loxP*
BVGC383	BVGC367	*his3Δ::FRT leu2Δ::FRT trp1Δ::FRT ura3Δ(-85+932)::Tn903NeoR ERG11::HIS3 PDR1::loxP*
BVGC387	BVGC367	*his3Δ::FRT leu2Δ::FRT trp1Δ::FRT ura3Δ(-85+932)::Tn903NeoR ERG11::HIS3* D1082G *PDR1::loxP*
BVGC391	BVGC367	*his3Δ::FRT leu2Δ::FRT trp1Δ::FRT ura3Δ(-85+932)::Tn903NeoR ERG11::HIS3 R376W PDR1::loxP*
BVGC361	BVGC340	*his3Δ::FRT leu2Δ::FRT trp1Δ::FRT ura3Δ(-85+932)::Tn903NeoR* Y141H S410F *ERG11::HIS3 PDR1::loxP*
BVGC365	BVGC361	*his3Δ::FRT leu2Δ::LEU2 trp1Δ::FRT ura3Δ(-*

38

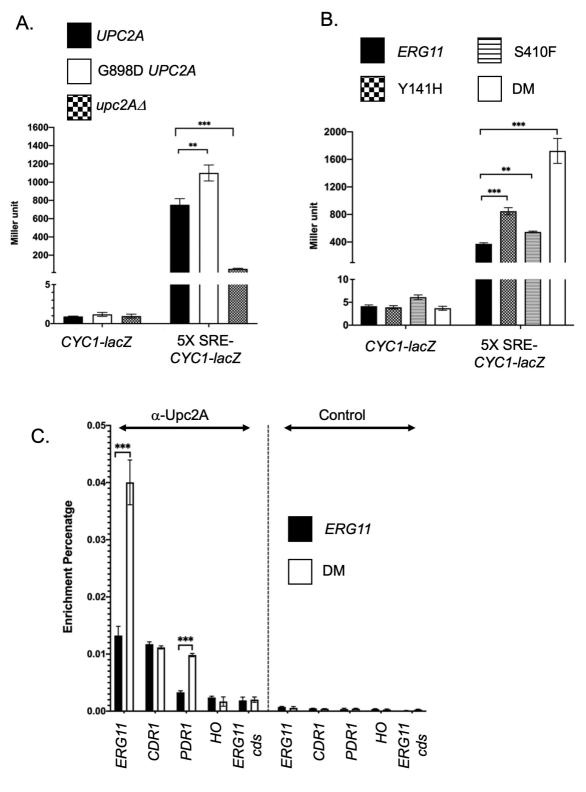|		
		85+932)::Tn903NeoR Y141H S410F ERG11::HIS3 PDR1-LOXP
BVGC374	BVGC344	*his3Δ::FRT leu2Δ::FRT trp1Δ::FRT ura3Δ(-85+932)::Tn903NeoR ERG11::HIS3 URA3::MET3-PDR1*
BVGC378	BVGC344	*his3Δ::FRT leu2Δ::FRT trp1Δ::FRT ura3Δ(-85+932)::Tn903NeoR ERG11::HIS3 URA3::MET3-UPC2A*
BVGC395	BVGC340	*his3Δ::FRT leu2Δ::FRT trp1Δ::FRT ura3Δ(-85+932)::Tn903NeoR Y141H S410F ERG11::HIS3 URA3::MET3-PDR1*
BVGC404	BVGC340	*his3Δ::FRT leu2Δ::FRT trp1Δ::FRT ura3Δ(-85+932)::Tn903NeoR Y141H S410F ERG11::HIS3 URA3::MET3-UPC2A*
BVGC511	BVGC344	*his3Δ::FRT leu2Δ::FRT trp1Δ::FRT ura3Δ(-*

		85+932)::Tn903NeoR ERG11::HIS3 crz1Δ::loxP
BVGC514	BVGC340	*his3Δ::FRT leu2Δ::FRT trp1Δ::FRT ura3Δ(-85+932)::Tn903NeoR* Y141H S410F *ERG11::HIS3 crz1Δ::loxP*

901

902   Table 1. Strains used in this work.

903

904

A.

Y141H

S410F

Conserved Positions in Erg11

B.

ERG11: wt, Y141H, S410F, DM

YPD | 20 μg/ml | 30 μg/ml
FLC

ERG11: wt, Y141H, S410F, DM

100 ng/ml | 150 ng/ml
CSF

ERG11: wt, Y141H, S410F, DM

1 μg/ml | 2 μg/ml
AmB

A. -FLC

B. +FLC, 3 hr

C. +FLC, 24 hr

D.

E. Caspofungin

A.

B.

C.

D.

A.

		SC	SC + methionine
ERG11	wt		
	DM		
MET3-UPC2A *ERG11*	Isolate #1		
	Isolate #2		
MET3-UPC2A DM *ERG11*	Isolate #1		
	Isolate #2		

B.

SC   SC+met
- - + +   - - + +   *MET3-UPC2A*
wt DM wt DM   wt DM wt DM   *ERG11*

Pdr1

Erg11

Upc2A

Tub

1 2 3 4   5 6 7 8

C.